Steady-State Polarization from Cylindrically Symmetric Fluorophores Undergoing Rapid Restricted Motion

Malcolm Irving
The Randall Institute, King's College London, London WC2B 5RL, England

ABSTRACT Steady-state fluorescence polarization measurements provide a relatively simple method for investigating the orientation of molecular components in ordered biological systems. However, the observed fluorescence polarization ratios also depend on any mobility of the fluorophores on the time scale of the fluorescence lifetime. Such mobility commonly arises from incomplete immobilization of a fluorescent probe on the macromolecule of interest. A theoretical formalism is presented for the interpretation of steady-state fluorescence polarization ratios in the presence of such rapid fluorophore motion. It is assumed that the fluorophores move freely within a cone between absorption and emission of a photon. Only one new parameter is introduced to describe fluorophore motion, the semi-angle of the cone, and this can be measured in separate experiments on an isotropic system. The fluorophore orientations are assumed to have cylindrical symmetry, but the symmetry axis need not be in the same plane as the center axes of the absorption and emission cones. This geometry applies to muscle and other biological fibers.

INTRODUCTION

Fluorescence polarization techniques are commonly used to study the mobility of macromolecules in solution and their orientation in ordered biological systems such as muscle and membranes (Weber, 1952; Weill and Sturm, 1975; Tregear and Mendelson, 1975; Yanagida and Oosawa, 1978; Axelrod, 1979). In time-resolved anisotropy decay measurements the motion of the fluorophore is studied on the time scale of the fluorescence or phosphorescence lifetime, and such measurements can be directly interpreted in terms of rotational diffusion coefficients and extents of angular motion for several experimental geometries (Kinosita et al., 1977; Lipari and Szabo, 1980; Burghardt, 1985).

Steady-state fluorescence polarization and dichroism measurements offer a technically less demanding method of monitoring fluorophore orientation in macroscopically ordered systems. Dichroism measurements are the simpler to interpret, because they depend only on the angular distribution of absorption dipoles. Fluorescence polarization ratios can give more information about the fluorophore orientation distribution but are also sensitive to motion of the fluorophores on the time scale of the fluorescence lifetime. Such motion may commonly be produced by the wobble of a fluorescent probe with respect to the macromolecule to which it is attached, or by flexibility in the local region of the macromolecule itself. The detailed effects of probe mobility depend on the experimental geometry: the symmetry of the fluorophore orientation distribution, and the relation of the direction of propagation of the exciting and fluorescent light and the absorption and emission dipoles to the symmetry axis. These effects have been calculated for specific observation geometries in membranes (Axelrod, 1979; Vogel and Jähnig, 1985) but have not been considered in steady-state fluorescence polarization measurements on cylindrically symmetric systems like muscle (Tregear and Mendelson, 1975; Yanagida and Oosawa, 1978; Wilson and Mendelson, 1983).

The present article derives analytical expressions for polarization ratios from mobile fluorophores under the simplifying assumption that the absorption and emission dipoles may each move freely within a cone on the time scale of the fluorescence lifetime. This introduces only one extra parameter to describe fluorophore motion: the semi-angle of the cone. In principle this parameter could be measured in separate experiments on an isotropic system. The center axes of the absorption and emission cones are not assumed to coincide in general. The fluorophore orientations are assumed to have cylindrical symmetry, but the symmetry axis need not be in the same plane as the center axes of the absorption and emission cones. The exciting light propagates at 90° to the symmetry axis, and fluorescence is observed along the same axis as the exciting light. This geometry applies to fluorescence polarization measurements from iodoacetamidotetramethylrhodamine covalently bound to myosin regulatory light chain in muscle fibres, as described in the accompanying papers (Ling et al., 1996; Allen et al., 1996). It could also be applied to other systems with the same experimental geometry.

Received for publication 12 September 1995 and in final form 10 January 1996.

Address reprint requests to Dr. Malcolm Irving, The Randall Institute, King's College London, 26-29 Drury Lane, London WC2B 5RL, England. Tel.: 44-71-8368851; Fax: 44-71-4979078; E-mail: udbp075@uk.ac.kcl.cc.bay.

0006-3495/96/04/1830/06 $2.00

THEORY

Single immobile fluorophore

The fluorophore has absorption dipole OA and emission dipole OE; the angle between them is μ (Fig. 1). The illumination and observation axes are assumed to be parallel and along Ox. Cylindrical symmetry will subsequently be

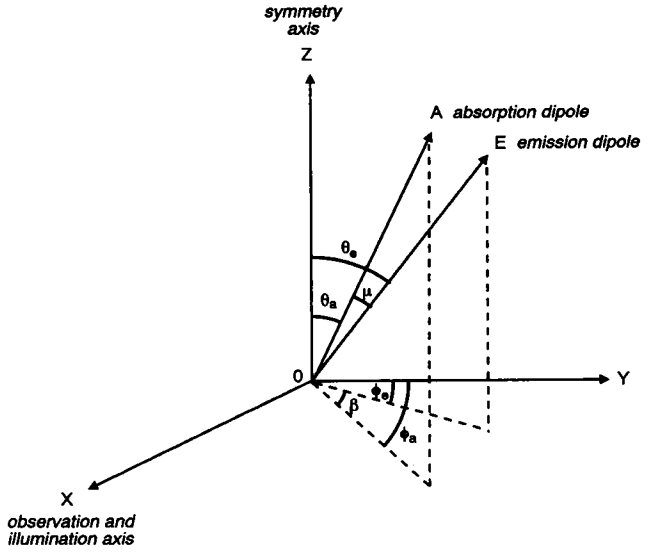

FIGURE 1 Angular coordinates of absorption (*OA*) and emission (*OE*) dipoles. The incident light is considered to propagate along *Ox* and the fluorescent light is observed along the same direction. The axial angles θ_a and θ_e are defined with respect to *Oz*, subsequently the symmetry axis. The corresponding azimuthal angles ϕ_a and ϕ_e are defined with respect to *Oy*, and the difference between them is β. The angle between the absorption and emission dipoles is μ.

imposed about *Oz*, so axial angles θ_a and θ_e are defined with respect to the *z* axis. Corresponding azimuthal angles ϕ_a and ϕ_e are defined with respect to *y*. Light polarized with its electric vector along *z* is referred to as the parallel (‖) component, and that with its electric vector along *y* as the perpendicular (⊥) component.

The probabilities of absorbing ‖ and ⊥ light components are given by, respectively,

$$p_{a\parallel} = k_1 \cos^2\theta_a \tag{1}$$

and

$$p_{a\perp} = k_1 \sin^2\theta_a \cos^2\phi_a, \tag{2}$$

where k_1 is a constant. Similarly, the emission probabilities are given by

$$p_{e\parallel} = k_2 \cos^2\theta_e \tag{3}$$

and

$$p_{e\perp} = k_2 \sin^2\theta_e \cos^2\phi_e, \tag{4}$$

where k_2 is a constant. Thus if ${}_mI_n$ denote the intensities of light components with excitation polarization *m* and emission polarization *n*, and *k* is a constant,

$${}_{\parallel}I_{\parallel} = k \cos^2\theta_a \cos^2\theta_e \tag{5}$$

$${}_{\parallel}I_{\perp} = k \cos^2\theta_a \sin^2\theta_e \cos^2\phi_e \tag{6}$$

$${}_{\perp}I_{\parallel} = k \sin^2\theta_a \cos^2\theta_e \cos^2\phi_a \tag{7}$$

$${}_{\perp}I_{\perp} = k \sin^2\theta_a \sin^2\theta_e \cos^2\phi_a \cos^2\phi_e. \tag{8}$$

Set of immobile fluorophores with cylindrical symmetry

With cylindrical symmetry about the *z* axis, the polarized fluorescence intensities from a set of fluorophores with uniform azimuthal distribution and axial angles θ_a and θ_e can be obtained by integrating Eqs. 5 to 8 with respect to ϕ_a, with $\phi_a - \phi_e$ constant (denoted by β, Fig. 1). After normalization, this gives

$${}_{\parallel}I_{\parallel} = k \cos^2\theta_a \cos^2\theta_e \tag{9}$$

$${}_{\parallel}I_{\perp} = \tfrac{1}{2}k \cos^2\theta_a \sin^2\theta_e \tag{10}$$

$${}_{\perp}I_{\parallel} = \tfrac{1}{2}k \sin^2\theta_a \cos^2\theta_e \tag{11}$$

$${}_{\perp}I_{\perp} = (k/8)\sin^2\theta_a \sin^2\theta_e (1 + 2\cos^2\beta) \tag{12}$$

(Tregear and Mendelson, 1975; Borejdo and Putnam, 1977).

Because absolute fluorescence intensities are difficult to obtain, the following intensity ratios (only three of which are independent) are normally calculated from experimental data:

$$P_{\parallel} = ({}_{\parallel}I_{\parallel} - {}_{\parallel}I_{\perp})/({}_{\parallel}I_{\parallel} + {}_{\parallel}I_{\perp}) \tag{13}$$

$$P_{\perp} = ({}_{\perp}I_{\perp} - {}_{\perp}I_{\parallel})/({}_{\perp}I_{\perp} + {}_{\perp}I_{\parallel}) \tag{14}$$

$$Q_{\parallel} = ({}_{\parallel}I_{\parallel} - {}_{\perp}I_{\parallel})/({}_{\parallel}I_{\parallel} + {}_{\perp}I_{\parallel}) \tag{15}$$

$$Q_{\perp} = ({}_{\perp}I_{\perp} - {}_{\parallel}I_{\perp})/({}_{\perp}I_{\perp} + {}_{\parallel}I_{\perp}). \tag{16}$$

Thus for a cylindrically symmetric set of immobile fluorophores,

$$P_{\parallel} = (3\cos^2\theta_e - 1)/(1 + \cos^2\theta_e) \tag{17}$$

$$P_{\perp} = \frac{(\sin^2\theta_e(1 + 2\cos^2\beta) - 4\cos^2\theta_e)}{(\sin^2\theta_e(1 + 2\cos^2\beta) + 4\cos^2\theta_e)} \tag{18}$$

$$Q_{\parallel} = (3\cos^2\theta_a - 1)/(1 + \cos^2\theta_a) \tag{19}$$

$$Q_{\perp} = \frac{(\sin^2\theta_a(1 + 2\cos^2\beta) - 4\cos^2\theta_a)}{(\sin^2\theta_a(1 + 2\cos^2\beta) + 4\cos^2\theta_a)} \tag{20}$$

Note that the expressions for *Q* are obtained from those for *P* by substituting θ_a for θ_e, and that only the parallel polarization ratios are independent of β.

Isotropic distribution of immobile fluorophores

For an isotropic distribution the only remaining variable is the angle between absorption and emission dipoles (μ), and

$${}_{\parallel}I_{\parallel}(\text{iso}) = {}_{\perp}I_{\perp}(\text{iso}) = (k/15)(1 + 2\cos^2\mu) \tag{21}$$

$${}_{\parallel}I_{\perp}(\text{iso}) = {}_{\perp}I_{\parallel}(\text{iso}) = (k/15)(2 - \cos^2\mu) \tag{22}$$

(Tregear and Mendelson, 1975; Borejdo and Putnam, 1977), hence

$$P_{\parallel} = P_{\perp} = P(\text{iso}) = (3\cos^2\mu - 1)/(3 + \cos^2\mu), \tag{23}$$

and the isotropic Q ratios are given by the same expression. If the absorption and emission dipoles are parallel ($\mu = 0$), P (iso) and Q (iso) take their maximum value of 0.5.

Mobility of fluorophores on the fluorescence time scale

The above calculations assumed no motion of the fluorophore between absorbing and emitting a photon. Such motion would produce fluorescence depolarization, as does a fixed angle between absorption and emission dipoles. However, if the motion is orientationally restricted, useful information about probe orientation or mobility can still be obtained from measured polarization ratios. The fluorophores are assumed to be uniformly distributed in a cone of semi-angle δ (Fig. 2). The axial and azimuthal angles of the cone axis are θ_{oa} and ϕ_{oa} for the absorption dipole and θ_{oe} and ϕ_{oe} for the emission dipole. Motion within the cone is considered to be rapid compared to the fluorescence lifetime, so that the orientation of the emission dipole within its cone at the moment of emission is independent of that of the absorption dipole at the moment of absorption. A useful special case is when the time- or ensemble-average orientation distributions of absorption and emission dipoles are identical. This will occur either if each fluorophore has parallel absorption and emission dipoles, or if the dipole orientation distributions are made equivalent by free rotation of the fluorophore within the cone.

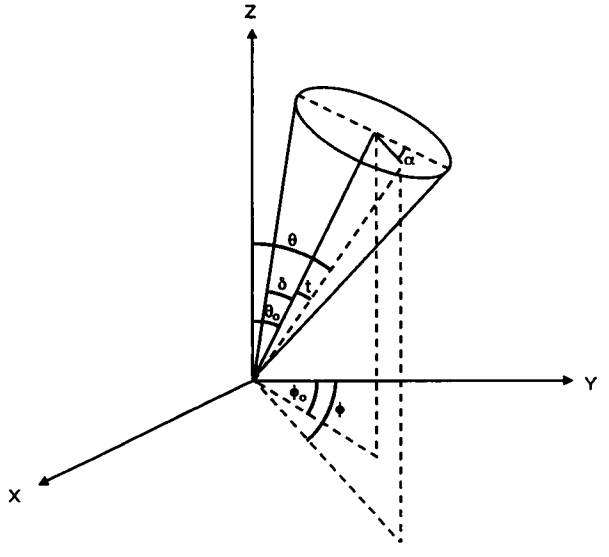

FIGURE 2 Angular coordinates of a cone in which the absorption or emission dipole of a fluorophore undergoes rapid motion. The axis of the cone has angular coordinates θ_o and ϕ_o in the coordinate system of Fig. 1. A general orientation within the cone has coordinates θ and ϕ in this system, and axial and azimuthal coordinates t and α with respect to the cone axis, where $\alpha = 0$ is taken in the plane defined by the cone axis and Oz. The outer limit of motion in the cone is given by $t = \delta$.

The general polarized intensity ${}_mI_n$ is given by

$$ {}_mI_n = \frac{\iint p_{am}(\theta_a, \phi_a)\, dV \iint p_{en}(\theta_e, \phi_e)\, dV}{(\iint dV)^2}, \qquad (24) $$

where the integrals are taken over the solid angle of the cone and p_{am} and p_{en} denote the probabilities of absorption and emission for polarizations m and n, respectively. Axial (t) and azimuthal (α) parametric coordinates for the cone are defined in Fig. 2. The general coordinates (θ, ϕ) for either absorption or emission dipoles are related to the cone axis coordinates (θ_o, ϕ_o) and parametric coordinates (t, α) by the equations

$$ \cos\theta = \cos t \cos\theta_o - \sin t \sin\theta_o \cos\alpha \qquad (25) $$

$$ \begin{aligned} \sin\theta\cos\phi = {} & \cos t \sin\theta_o \cos\phi_o \\ & + \sin t \cos\alpha \cos\theta_o \cos\phi_o \\ & - \sin t \sin\alpha \sin\phi_o \end{aligned} \qquad (26) $$

$$ \begin{aligned} \sin\theta\sin\phi = {} & \cos t \sin\theta_o \sin\phi_o \\ & + \sin t \cos\alpha \cos\theta_o \sin\phi_o \\ & + \sin t \sin\alpha \cos\phi_o. \end{aligned} \qquad (27) $$

From Eq. 24:

$$ {}_{\|}I_{\|} = \frac{\iint p_{a\|}(\theta_a, \phi_a)\, dV \iint p_{e\|}(\theta_e, \phi_e)\, dV}{(\iint dV)^2} \qquad (28) $$

and

$$ \iint p_{a\|}(\theta_a, \phi_a)\, dV $$

$$ = \int_{\alpha=0}^{2\pi}\int_{t=0}^{\delta} k_1 \cos^2\theta_a \sin t\, dt\, d\alpha $$

$$ = \int_{\alpha=0}^{2\pi}\int_{t=0}^{\delta} k_1 (\cos t \cos\theta_{oa} - \sin t \sin\theta_{oa}\cos\alpha)^2 \sin t\, dt\, d\alpha $$

$$ = [2\pi(1 - \cos\delta)]\tfrac{1}{2}k_1(\omega + (2 - 3\omega)\cos^2\theta_{oa}), \qquad (29) $$

where

$$ \omega = 1 - (1 + \cos\delta + \cos^2\delta)/3 \qquad (30) $$

A similar expression is obtained for $\iint p_{e\|}(\theta_e, \phi_e)\, dV$, except that the constant k_2 replaces k_1 (cf. Eqs. 1 and 3), and $\cos^2\theta_{oe}$ replaces $\cos^2\theta_{oa}$.

Because

$$ \iint dV = \int_{\alpha=0}^{2\pi}\int_{t=0}^{\delta} \sin t\, dt\, d\alpha = [2\pi(1 - \cos\delta)], $$

the solid angle of the cone,

$$ {}_{\parallel}I_{\parallel} = \tfrac{1}{4}k(\omega + (2 - 3\omega)\cos^2\theta_{oa}) \times (\omega + (2 - 3\omega)\cos^2\theta_{oe}). \quad (31) $$

Because this equation is independent of ϕ, it also applies to a cylindrically symmetric set of fluorophores with the same axial angle distribution. It reduces to Eq. 5 when $\delta = 0$, $\omega = 0$.

Similarly,

$$ {}_{\parallel}I_{\perp} = \frac{\iint p_{a\parallel}(\theta_a, \phi_a)\, dV \iint p_{e\perp}(\theta_e, \phi_e)\, dV}{(\iint dV)^2}, \quad (32) $$

where

$$ \iint p_{e\perp}(\theta_e, \phi_e)\, dV = \int_{\alpha=0}^{2\pi}\int_{t=0}^{\delta} k_2 \sin^2\theta_e \cos^2\phi_e \sin t\, dt\, d\alpha. $$

Substituting from Eq. 26 and integrating:

$$ \iint p_{e\perp}(\theta_e, \phi_e)\, dV \quad (33) $$

$$ = [2\pi(1 - \cos\delta)](k_1/2)\{\omega + (2 - 3\omega)\sin^2\theta_{oe}\cos^2\phi_{oe}\}. $$

Substituting Eqs. 29 and 33 in Eq. 32, normalizing, and averaging over azimuthal angle for cylindrical symmetry, one obtains

$$ {}_{\parallel}I_{\perp} = (k/8)[(\omega + (2 - 3\omega)\cos^2\theta_{oa}] \times [2\omega + (2 - 3\omega)\sin^2\theta_{oe}]. \quad (34) $$

Combining Eqs. 31 and 34:

$$ P_{\parallel} = \frac{(2 - 3\omega)\,(3\cos^2\theta_{oe} - 1)}{4\omega + (2 - 3\omega)\,(1 + \cos^2\theta_{oe})} \quad (35) $$

(see Fig. 3 in Results).

Similarly,

$$ {}_{\perp}I_{\parallel} = (k/8)[2\omega + (2 - 3\omega)\sin^2\theta_{oa}] \times [\omega + (2 - 3\omega)\cos^2\theta_{oe}]. \quad (36) $$

Combining Eqs. 31 and 36:

$$ Q_{\parallel} = \frac{(2 - 3\omega)\,(3\cos^2\theta_{oa} - 1)}{4\omega + (2 - 3\omega)\,(1 + \cos^2\theta_{oa})}. \quad (37) $$

Finally,

$$ {}_{\perp}I_{\perp} = \frac{\iint p_{a\perp}(\theta_a, \phi_a)\, dV \iint p_{e\perp}(\theta_e, \phi_e)\, dV}{(\iint dV)^2} \quad (38) $$

Writing $\beta_o = \phi_{oa} - \phi_{oe}$, this gives

$$ {}_{\perp}I_{\perp} = (k/32)\{(1 + 2\cos^2\beta_o)C(\theta_{oa}, \theta_{oe}, \omega) + (1 + 2\sin^2\beta_o)S(\theta_{oa}, \theta_{oe}, \omega)\}, \quad (39) $$

where

$$ C(\theta_{oa}, \theta_{oe}, \omega) = [\omega + (2 - 3\omega)\sin^2\theta_{oa}] \times [\omega + (2 - 3\omega)\sin^2\theta_{oe}] + \omega^2 \quad (40) $$

and

$$ S(\theta_{oa}, \theta_{oe}\, \omega) = \omega\{[\omega + (2 - 3\omega)\sin^2\theta_{oa}] + [\omega + (2 - 3\omega)\sin^2\theta_{oe}]\}. \quad (41) $$

If the absorption and emission dipoles are effectively parallel for the fluorophore distribution, so that $\theta_{oa} = \theta_{oe}$, $\phi_{oa} = \phi_{oe}$ and $\beta_o = 0$, Eqs. 39 to 41 reduce to

$$ {}_{\perp}I_{\perp} = (k/32)\{3[\omega + (2 - 3\omega)\sin^2\theta_o]^2 + 3\omega^2 + 2\omega[\omega + (2 - 3\omega)\sin^2\theta_o]\}. \quad (42) $$

$P_{\perp}$ and $Q_{\perp}$ are obtained from Eq. 39 or 42 and Eq. 34 or 36 (see Fig. 4 in Results).

In practice it is unlikely that all fluorophores in a sample have exactly the same orientation. In the general case polarization ratios can be obtained by integrating Eqs. 31, 34, 36, and 39 over the angular distribution of θ_{oa} and θ_{oe}.

Isotropic distribution of fluorophores

The intensities of polarized light components for an isotropic distribution of fluorophores can be calculated for the general case starting from Eqs. 5 to 8. The angle μ between the axes of the absorption and emission cones is a constant, but for any absorption cone axis (θ_a, ϕ_a) the emission cone axis may take a range of orientations (θ_e, ϕ_e) tracing out another cone with semi-angle μ. Integrating over possible orientations of absorption and emission dipoles, keeping μ constant, gives, for an isotropic distribution,

$$ {}_{\parallel}I_{\parallel}(\text{iso}) = {}_{\perp}I_{\perp}(\text{iso}) = (k/60)[5\omega(4 - 3\omega) + (2 - 3\omega)^2(1 + 2\cos^2\mu)] \quad (43) $$

$$ {}_{\parallel}I_{\perp}(\text{iso}) = {}_{\perp}I_{\parallel}(\text{iso}) = (k/60)[5\omega(4 - 3\omega) + (2 - 3\omega)^2(2 - \cos^2\mu)] \quad (44) $$

$$ P(\text{iso}) = Q(\text{iso}) = \frac{(2 - 3\omega)^2(3\cos^2\mu - 1)}{10\omega(4 - 3\omega) + (2 - 3\omega)^2(3 + \cos^2\mu)} \quad (45) $$

(see Fig. 5 in Results).

If the absorption and emission dipoles are effectively parallel, $\mu = 0$ and

$$ {}_{\parallel}I_{\parallel}(\text{iso}) = {}_{\perp}I_{\perp}(\text{iso}) = (k/15)\,(3\omega^2 - 4\omega + 3) \quad (46) $$

$$ {}_{\parallel}I_{\perp}(\text{iso}) = {}_{\perp}I_{\parallel}(\text{iso}) = (k/30)\,(-3\omega^2 + 4\omega + 2) \quad (47) $$

$$ P(\text{iso}) = Q(\text{iso}) = (2 - 3\omega)^2/(3\omega^2 - 4\omega + 8). \quad (48) $$

RESULTS AND DISCUSSION

The general effect of rapid fluorophore mobility is to decrease the amplitude of the observed polarization ratios. Fig. 3 shows the dependence of $P_{\parallel}$ on the axial angle of the emission dipole cone axis (θ_{oe}) for four values of δ, the semi-angle of the wobble cone (Eq. 35). $\delta = 0$ gives the immobile dipole result (Eq. 17). As δ is increased the amplitude of $P_{\parallel}$ decreases, but a positive value of $P_{\parallel}$ always indicates that θ_{oe} is less than 54.7°. When $\delta = 90°$ the cone occupies all angular space and $P_{\parallel}$ is zero. $Q_{\parallel}$ has the same dependence on δ (Eq. 37), except that θ_{oe} is replaced by θ_{oa}. The effect of rapid fluorophore mobility on $P_{\parallel}$ and $Q_{\parallel}$ is in marked contrast to that of a fixed angle between immobile absorption and emission dipoles, which has no effect on $P_{\parallel}$ and $Q_{\parallel}$, apart from their respective dependence on θ_{oe} and θ_{oa} (Eqs. 17 and 19). In general a systematic offset between absorption and emission dipoles produces a difference between $P_{\parallel}$ and $Q_{\parallel}$. Conversely, if $P_{\parallel} = Q_{\parallel}$, θ_{oe} must equal θ_{oa}.

The effect of fluorophore mobility on $P_{\perp}$ is shown in Fig. 4 *A* for the same four values of δ, for no systematic offset between absorption and emission dipoles. The general effect of increasing δ is roughly similar to that on $P_{\parallel}$ (Fig. 3), but the value of θ_o at which $P_{\perp} = 0$ increases with increasing δ. A positive value of $P_{\perp}$ indicates that θ_o is greater than 49.1°. The effect of fluorophore mobility is again qualitatively different from that of a systematic offset between absorption and emission dipoles, shown in Fig. 4 *B* for four different values of β, the azimuthal component of the angular offset. An increase in β always leads to a decrease in $P_{\perp}$ (Fig. 4 *B*), whereas an increase in δ leads to an increase in $P_{\perp}$ at small θ (Fig. 4 *A*).

Both rapid fluorophore motion (within a cone of semi-angle δ) and a fixed angle (μ) between absorption and emission dipoles lead to a decrease in the polarization ratio P(iso) observed for an isotropic distribution of fluorophores

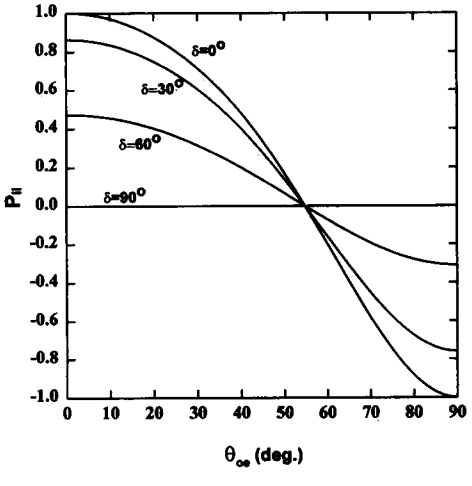

FIGURE 3 Dependence of $P_{\parallel}$ on the axial angle of the emission dipole cone axis (θ_{oe}) for four values of δ, the semi-angle of the cone in which the dipole moves freely on the fluorescence time scale. $\delta = 0$ corresponds to the immobile dipole case.

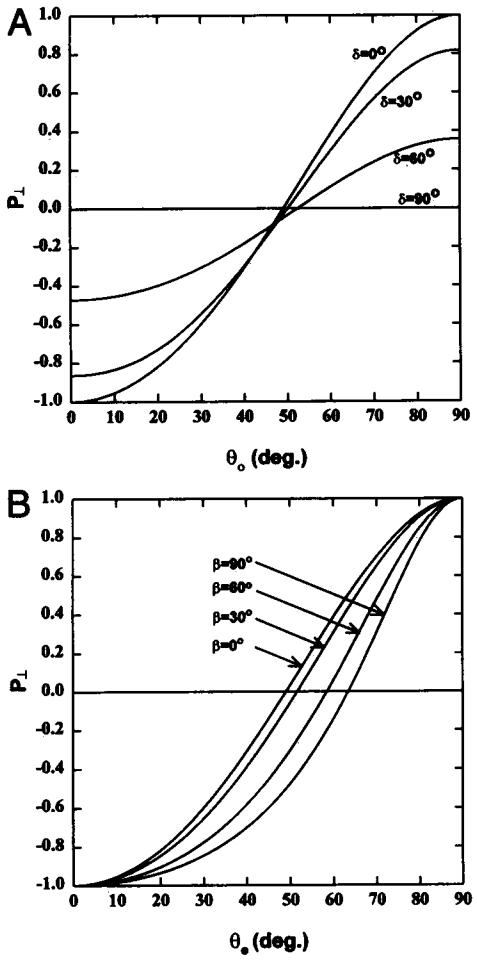

FIGURE 4 Dependence of $P_{\perp}$ on the axial angle of the emission dipole. (*A*) No fixed offset between absorption and emission dipoles, but free movement in a cone of semi-angle δ between absorption and emission. θ_o denotes the angle between the cone axis and the z axis. $\delta = 0$ corresponds to the immobile dipole case. (*B*) Fixed azimuthal angle β (defined in Fig. 1) between absorption and emission dipoles, but no motion on the fluorescence time scale. θ_e denotes the angle between the emission dipole axis and the z axis.

(Fig. 5). For small angles the effect of motion within a cone of semi-angle δ with $\mu = 0$ (Fig. 5, *dashed line*) is numerically equivalent to that of a fixed offset (Fig. 5, *continuous line*, $\delta = 0$) μ between absorption and emission dipoles. However, the relations diverge at larger angles, and negative values of P(iso) can only be produced by large values of μ.

The formalism presented above extends previous treatments of steady-state polarization from cylindrically symmetric immobile fluorophores (Tregear and Mendelson, 1975; Yanagida and Oosawa, 1978; Wilson and Mendelson, 1983) to the more general case in which restricted motion of the fluorophores may take place on a time scale shorter than the fluorescence lifetime. Examples of the application of this approach are presented in the accompanying papers (Ling et al., 1996; Allen et al., 1996). Such fluorophore motion is likely whenever a small probe is covalently teth-

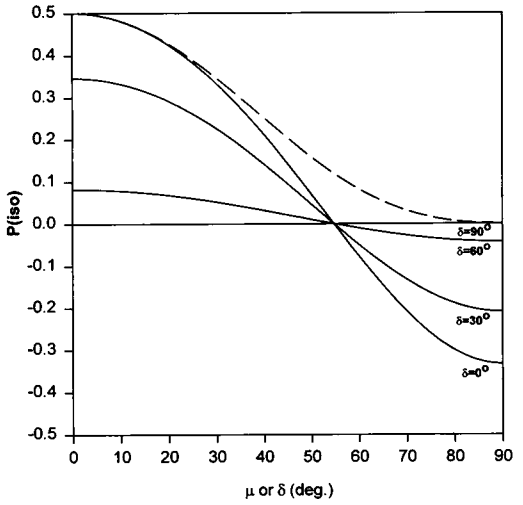

FIGURE 5 Dependence of the isotropic polarization ratio P(iso) on the angle between absorption and emission dipoles (μ) for four values of δ, the semi-angle of the cone in which the dipole moves freely on the fluorescence time scale (*continuous lines*), and on δ for the case of no fixed offset between absorption and emission dipoles ($\mu = 0$; *dashed line*).

ered to a single point on the surface of a macromolecule, and is routinely considered in time-resolved anisotropy measurements (e.g., Kinosita et al., 1977; Lipari and Szabo, 1980; Burghardt, 1985), in which different temporal components of probe motion can be directly measured. These components cannot be characterized by steady-state polarization measurements, but the formalism presented here shows that the effects of a rapid but restricted motion on such measurements can be represented by a single additional parameter, δ, the semi-angle of a cone in which the probe wobbles freely. δ can be conveniently determined by measuring polarization ratios for an isotropic distribution of fluorophores (Fig. 5), provided that the fixed offset between absorption and emission dipoles is known.

In addition to motion on a time scale shorter than the fluorescence lifetime, real fluorophores are likely to undergo slower motions or have static orientational disorder. Steady-state fluorescence polarization measurements cannot distinguish between such slow motions and static disorder. Thus in interpreting these measurements it is convenient to partition the orientational disorder into "dynamic" and "static" components, meaning fast and slow compared to the fluorescence lifetime. Motions on a time scale similar to the fluorescence lifetime will contribute to both components and can only be fully characterized by time-resolved measurements. With this definition and limitation, the contribution of dynamic disorder to steady-state fluorescence measurements can be analyzed by the wobble-in-a-cone model formalism presented above. Static disorder can be accommodated by integrating the results for a single axial angle (Eqs. 31, 34, 36, and 39 above) over the axial orientation distribution of interest (Ling et al., 1996; Allen et al., 1996).

Dynamic and static disorder have markedly different effects on the measured polarization ratios. If the dynamic disorder is very large the measured polarization ratios will approach a value of zero (Figs. 3 and 4 *A*), but when the static disorder is very large (approaching an isotropic distribution) the polarization ratios approach a limiting value of 0.5 if the absorption and emission dipoles are parallel (Fig. 5). Previous interpretations of steady-state polarization ratios from cylindrically symmetric fluorophores (Tregear and Mendelson, 1975; Yanagida and Oosawa, 1978; Wilson and Mendelson, 1983) have taken into account static but not dynamic disorder. The effects of the latter cannot be accurately reproduced by allowing a variable offset between absorption and emission dipoles, because dynamic disorder affects both the parallel and perpendicular polarization ratios, whereas an offset between absorption and emission dipoles directly affects only the perpendicular ratios (Figs. 3 and 4). If the effects of dynamic disorder are neglected, conclusions about the average axial orientation distribution of fluorophores may be unreliable.

I am grateful to Drs. R. E. Dale and Y. E. Goldman for critical comments on an earlier version of the manuscript.

I am also grateful to the Wellcome Trust and Royal Society for financial support.

REFERENCES

Allen, T. St. C., N. Ling, M. Irving, and Y. E. Goldman. 1996. Orientation changes in myosin regulatory light chains following photorelease of ATP in skinned muscle fibers. *Biophys. J.* 70:000–000.

Axelrod, D. 1979. Carbocyanine dye orientation in red cell membrane studied by microscopic fluorescence polarization. *Biophys. J.* 26: 557–574.

Borejdo, J., and S. Putnam. 1977. Polarization of fluorescence from single skinned glycerinated rabbit psoas fibers in rigor and relaxation. *Biochim. Biophys. Acta.* 459:578–595.

Burghardt, T. P. 1985. Time-resolved fluorescence polarization from ordered biological assemblies. *Biophys. J.* 48:623–631.

Kinosita, K., S. Kawato, and A. Ikegami. 1977. A theory of fluorescence polarization decay in membranes. *Biophys. J.* 20:289–305.

Ling, N., C. Shrimpton, J. Sleep, J. Kendrick-Jones, and M. Irving. 1996. Fluorescent probes of the orientation of myosin regulatory light chains in relaxed, rigor, and contracting muscle. *Biophys. J.* 70:000–000.

Lipari, G., and A. Szabo. 1980. Effect of librational motion on fluorescence depolarization and nuclear magnetic resonance relaxation in macromolecules and membranes. *Biophys. J.* 30:489–506.

Tregear, R. T., and R. M. Mendelson. 1975. Polarization from a helix of fluorophores and its relation to that obtained from muscle. *Biophys. J.* 15:455–467.

Vogel, H., and F. Jähnig. 1985. Fast and slow orientational fluctuations in membranes. *Proc. Natl. Acad. Sci. USA.* 82:2029–2033.

Weber, G. 1952. Polarization of the fluorescence of macromolecules. *Biochem. J.* 51:145–155.

Weill, G., and J. Sturm. 1975. Polarized fluorescence in an electric field. A model calculation with application to the geometry of the 2-hydroxy-4,4′-diamidinostilbene-DNA complex. *Biopolymers.* 14:2537–2553.

Wilson, M. G. A., and R. M. Mendelson. 1983. A comparison of order and orientation of crossbridges in rigor and relaxed muscle fibres using fluorescence polarization. *J. Muscle Res. Cell Motil.* 4:671–693.

Yanagida, T., and F. Oosawa. 1978. Polarized fluorescence from ϵ-ADP incorporated into F-actin in a myosin-free single fiber: conformation of F-actin and changes induced in it by heavy meromyosin. *J. Mol. Biol.* 126:507–524.